European Journal of Radiology 113 (2019) 158–164

Contents lists available at ScienceDirect

European Journal of Radiology

journal homepage: www.elsevier.com/locate/ejrad

Research article

Marrow adiposity as an indicator for insulin resistance in postmenopausal women with newly diagnosed type 2 diabetes – an investigation by chemical shift-encoded water-fat MRI

Lequn Zhu[a,1], Zheng Xu[b,1], Guanwu Li[a,*], Ying Wang[c], Xuefeng Li[a], Xiao Shi[d], Haiyang Lin[e], Shixin Chang[a]

[a] Department of Radiology, Yueyang Hospital of Integrated Traditional Chinese and Western Medicine, Shanghai University of Traditional Chinese Medicine, Shanghai 200437, China
[b] Xinzhuang Community Health Center, Shanghai 201199, China
[c] Department of Clinical Laboratory, Yueyang Hospital of Integrated Traditional Chinese and Western Medicine, Shanghai University of Traditional Chinese Medicine, Shanghai 200437, China
[d] Department of Geriatrics, Yueyang Hospital of Integrated Traditional Chinese and Western Medicine, Shanghai University of Traditional Chinese Medicine, Shanghai 200437, China
[e] Department of Endocrinology, The Affiliated Wenling Hospital, Wenzhou medical University, Zhejiang 317500, China

ARTICLE INFO

Keywords:
Type 2 diabetes
Chemical shift imaging
Bone marrow
Insulin resistance

ABSTRACT

Background: Marrow fat accumulates in diabetic conditions but remains elusive. The published works on the relationships between marrow fat phenotypes and glucose homeostasis are controversial.
Purpose: To detect the association of insulin resistance with marrow adiposity in postmenopausal women with newly diagnosed type 2 diabetes (T2D) using chemical shift-encoded water–fat MRI.
Methods: We measured vertebral proton density fat fraction (PDFF) by 3T-MRI in 75 newly diagnosed T2D and 20 nondiabetic postmenopausal women. Bone mineral density (BMD), whole body fat mass and lean mass were determined by dual-energy X-ray absorptiometry. Insulin sensitivity was estimated using the homeostasis model assessment of insulin resistance (HOMA-IR).
Results: Lumbar spine PDFF was higher in women with T2D (65.9 ± 6.8%) than those without diabetes (59.5 ± 6.1%, $P = 0.009$). There was a consistent inverse association between the vertebral PDFF and BMD. PDFF had a positive association with glycated hemoglobin and HOMA-IR but not with fasting plasma glucose and insulin. PDFF was significantly increased, and BMD was decreased in a linear trend from the lowest (< 1.90) to highest (≥2.77) HOMA-IR quartile. Multivariate linear regression analyses revealed a positive association between log-transformed HOMA-IR and PDFF after adjustment for multiple covariates (ß = 0.382, $P < 0.001$). The positive association of HOMA-IR with PDFF remained robust when total body lean mass and fat mass, BMD was entered into the multivariate regression model, respectively (ß = 0.293 and ß = 0.251, respectively; all $P < 0.05$).
Conclusions: Elevated HOMA-IR was linked to higher marrow fat fraction in postmenopausal women with newly diagnosed T2D independently of body compositions.

1. Introduction

Diabetes may negatively impact skeletal integrity by unbalancing several pathways such as bone formation, bone resorption, marrow adipogenesis, collagen formation, secretion of inflammatory cytokine, and calcium metabolism, etc. [1,2]. Hyperinsulinemia and insulin

Abbreviations: BMD, bone mineral density; BMI, body mass index; CSE, chemical shift-encoded; DXA, dual-energy X-ray absorptiometry; HbA1c, glycosylated hemoglobin; HDL, high-density lipoprotein; HOMA-IR, homeostasis model assessment of insulin resistance; LDL, low-density lipoprotein; METs, metabolic equivalent of tasks; PDFF, proton density fat fraction; ROI, region of interest; SD, standard deviation; TE, Echo time; T2D, Type 2 diabetes; TR, repetition time

* Corresponding author at: Department of Radiology, Yueyang Hospital of Integrated Traditional Chinese and Western Medicine, Shanghai University of Traditional Chinese Medicine, 110 Ganhe Rd, Shanghai 200437, China.
E-mail address: purenyi@163.com (G. Li).
[1] Zheng Xu and Lequn Zhu contributed equally to this study as co-first author.

https://doi.org/10.1016/j.ejrad.2019.02.020
Received 19 October 2018; Received in revised form 14 January 2019; Accepted 15 February 2019

resistance are the hallmarks of type 2 diabetes (T2D). Despite higher or normal bone mineral density (BMD), T2D populations have increased fracture risk as compared with non-diabetic subjects [3,4]. These paradoxical findings might be ascribed to the impact of insulin resistance on skeletal integrity, but the associations of insulin resistance with bone structure and material properties remain elusive.

Marrow adipose tissue is considered as an insulin-sensitive tissue and has shown surprising effects on other adipose tissue depots and whole body energy metabolism, because of the expression of genetic and metabolic traits of brown adipose tissue [5,6]. Several studies investigated marrow adiposity in T2D with conflicting results, showing T2D populations have higher marrow fat content [3] or no significant differences [7–9] compared to those without diabetes. Similarly, the effects of hyperinsulinemia and insulin resistance on bone health are not fully understood, and the published studies on the relationships between marrow fat phenotypes and glucose homeostasis have been inconclusive. Insulin resistance had a positive [10], negative [11] or no [9,12,13] association with marrow fat expansion. Challenges to interpreting currently available data arising from inhomogeneous cohorts with secondary factors affecting bone health, relatively small sample size, and use of diverse measurements such as homeostasis model assessment of insulin resistance (HOMA-IR), fasting insulin and glucose.

Since marrow adipocytes express insulin receptors and respond to insulin-sensitizing anti-diabetic thiazolidinedione, marrow adipose tissue is under the effect of systemic insulin [14]. In addition, animal studies have shown that marrow fat volume is not linked directly to peripheral fat accumulation and, instead, is coincident with insulin resistance [15]. The present study aimed to test the hypothesis that marrow fat expansion had a positive association with insulin resistance in postmenopausal women with newly diagnosed T2D using chemical shift-encoded (CSE) water-fat MRI.

2. Material and methods

2.1. Study participants

In this cross-sectional study, eighty postmenopausal women with newly diagnosed T2D who were older than 50 years with more than 1 year since menopause and had not previously received any anti-diabetes medication, and 20 age- and body mass index (BMI)-matched healthy controls were recruited between March 2013 and May 2018. None of the volunteers met any of the other exclusion criteria. The definition of diabetes was based on the American Diabetes Association guidelines and in the presence of fasting plasma glucose levels of 7.0 mmol/L or higher (126 mg/dL), 2-hour plasma glucose of 11.1 mmol/L or higher (200 mg/dL), glycated hemoglobin (HbA1c) of 6.5% or higher.

The key exclusion criteria were as follows: 1) history of medical disorders known to affect bone and fat metabolism except for T2D, such as previous or current malignant tumor, exposure to chemo-radiotherapy, chronic renal and liver disease, pituitary or hypothalamic disorders, parathyroid disease or vitamin D deficiency, or other chronic illnesses; 2) any prior or current use of drugs that could affect fat and bone metabolism, such as systemic hormonal replacement therapy, bisphosphonates, glucocorticoids, proton pump inhibitors; 3) any confounder that had the potential to interfere with the interpretation of the findings, such as lumbar spine or hip fracture; and 4) contraindications to MRI examination. All women completed questionnaires about medical history and medication use. After implementation of the exclusion criteria, five T2D women with vertebral hemangiomas and silent compression fractures were excluded from the current study. Therefore, our analytical sample size for this study was 95. Study procedures were in accordance with institutional guidelines and approved by an Institutional Review Board. Informed consent was obtained from all participants before enrolling them into study.

2.2. Lifestyle factors and anthropometric measurements

All participants underwent a thorough physical examination. Age, years since menopause, body weight, height, smoking history, drinking habits, physical activity, and calcium and phosphorus intake were recorded. Body weight and height were obtained using standard protocols and were measured to the nearest 0.1 kg and 0.5 cm, respectively. BMI was calculated from the body weight and height. Smoking was categorized as never, past or current, and alcohol consumption was defined as at least one alcoholic beverage per day. Physical activity was assessed using the International Physical Activity Questionnaire short form, with data reported as Metabolic Equivalent of Task hours per week [16].

2.3. Biochemical measurements

Blood samples were collected via a cubital vein puncture under standard conditions between 7 a.m. and 9 a.m. after at least 12-h overnight fasting. The fasting plasma concentrations of glucose, insulin, HbA1c, and lipids profile including total cholesterol, triglycerides, high- and low-density lipoprotein cholesterol were measured according to standard laboratory methods at the Central Laboratory. HOMA-IR was calculated from levels of fasting plasma insulin and glucose by using HOMA Calculator Software (the University of Oxford), with higher values indicating insulin resistance. Quartiles for the cohort distribution for the HOMA-IR were as follows: Quartile 1, < 1.90; Quartile 2, 1.90–2.19; Quartile 3, 2.20–2.76; and Quartile 4, ≥ 2.77.

2.4. BMD and non-bone body composition measurements

Areal BMD (g/cm^2) at the total hip, femoral neck and lumbar spine (from L1 to L4) was assessed using dual-energy X-ray absorptiometry (DXA, Prodigy Lunar, GE Healthcare, Waukesha, WI). Whole body lean mass and fat mass were measured from total body DXA scans. All measurements were done by the same of accredited technician using a standard operating procedure. The scanner was checked daily before each scanning session using the GE Lunar calibration phantom, as recommended by the manufacturer to control possible baseline drift. The coefficient of variations of BMD at the lumbar spine, femoral neck and total hip, total body fat mass and lean mass measurements were less than 1.19%.

2.5. MR image acquisition

Scans were acquired using a 3-T scanner (Ingenia, Philips Healthcare, Best, the Netherlands). The images were acquired with subject in the supine position using the standard spine-array receive coil. MRI acquisition included standard clinical sagittal T1- and T2-weighted images for morphological assessments of the lumbar region.

CSE–MRI was performed to obtain the proton density fat fraction (PDFF) of the lumbar spine using an eight-echo 3D spoiled gradient echo sequence in the spine sagittal plane as described previously [17]. The sequence acquired eight echoes in a single repetition time (TR) using mono-flyback read-out gradients. The imaging parameters were as following: TR = 10 ms, echo time $(TE)_{init}/\Delta TE = 1.48/1.2$ ms, field of view = 400 mm × 400 mm, frequency direction = A/P (to minimize breathing artifacts), matrix = 256 × 256, slice thickness = 3 mm, flip angle = 3°(given the large T1 difference between water and fat components in the bone marrow [18], a small excitation flip angle was used to minimize T1-bias effects) [19–21]; receiver bandwidth = 1.3 kHz/pixel, and number of signals averaged = 1.

Accounting for the water/fat separation strongly depends on the initial guess of the B0 inhomogeneity map, we first performed a region-growing algorithm to evaluate the field-map variation according to the method as previously described [17,22]. In order to enable a robust water–fat separation, phase errors induced by echo misalignments, the

concomitant gradient field and a constant phase offset between time-interleaves echo trains were corrected [20,23]. A complex-based water–fat decomposition was then performed using a single T2* correction and a pre-calibrated eight-peak spectral model of fat, considering the presence of the multiple peaks in the fat spectrum [24]. The pre-calibrated fat spectrum was modeled by using the bone marrow fat spectrum at the lumbar spine characterized by Karampinos et al. [25] and Dieckmeyer et al. [26], but not the choice of the liver fat spectrum. Image reconstructions yielded quantitative PDFF maps, defining the ratio of the fat signal over the sum of fat and water signals. The PDFF maps were exported to an OsiriX DICOM viewer to manually draw regions of interest (ROIs) by two independent radiologists. Three ROI measurements were made from the three most central slices depicting each vertebra (from L1 to L4), as large as possible on midline sagittal images and were excluded from the cortical bone and endplates. We calculated Lin's concordance correlation coefficient and intra-class correlation coefficient to assess the inter-rater agreement regarding the PDFF measures. The mean PDFF values obtained by both raters were averaged for final statistical analysis. More details of the image acquisition and analysis have been previously described. [17]

2.6. Statistical analysis

Data are presented as means ± SD, median (interquartile range) or frequency (%) as appropriate. We analyzed constitutive variables with a Student *t* test or non-parametric test and categorical variables with a Chi-squared test between the T2D and control groups. Trends in clinical characteristics of the T2D group across HOMA-IR quartiles were examined using Polynomial test for continuous variables and Linear by Linear association test for categorical variables. The least square mean values of PDFF or BMD were compared across quartiles of HOMA-IR after controlling for age, BMI, alcohol intake, tobacco use, physical activity, serum lipids profile, whole body fat mass, lean mass and BMD for PDFF comparisons or PDFF for BMD comparisons, and then a multiple linear regression analysis was performed to test for a linear trend. *Pearson*'s and *Spearman*'s correlations for normally and non-normally distributed, respectively, were used to detect the associations among the PDFF, BMD and insulin resistance indicators or hormones involved in the metabolism of glucose. To evaluate the independent association of PDFF with HOMA-IR, we performed multivariate regression analyses after adjustment for potential covariates, including age, BMI, alcohol intake, tobacco use, physical activity and serum lipids profile in model 1. Model 2 was also adjusted for whole body fat mass and lean mass. Finally, model 3 was additionally adjusted for bone mass. Due to skewed distribution, variables such as HOMA-IR were entered to model as log-transformed unit. Statistical analyses were performed with IBM SPSS Statistics for Mac OS (Version 23.0. Armonk, NY) and the level of significance was set at $\alpha = 0.05$.

3. Results

3.1. Baseline characteristics

The baseline characteristics of the study populations are represented in Table 1. There was no significant difference between the two groups except for HbA1c and glucose levels, as expected and also levels of triglyceride and high-density lipoprotein. We performed a subgroup analysis for the T2D women according to the quartiles of HOMA-IR (Table 1). Increasing trend was observed in the mean body weight, BMI, total body fat mass and lean mass, levels of triglyceride, high-density lipoprotein cholesterol, fasting blood glucose, insulin, and HbA1c from the lowest to highest HOMA-IR quartile ($P < 0.05$ for all). The mean age, height, physical activity, alcohol intake, history of smoking, total cholesterol, and low-density lipoprotein cholesterol did not differ significantly among HOMA-IR quartiles.

3.2. Inter-rater reliability for the PDFF measurements

The Lin's concordance correlation coefficient was 0.961 (95% confidence interval [CI], 0.944–0.983), and intra-class correlation coefficient was 0.980 (95% CI, 0.963–0.995) as measured for the inter-rater agreement, suggesting an excellent agreement between the two observers for the PDFF measurements.

3.3. PDFF and BMD across HOMA-IR quartiles

Lumbar spine PDFF was higher in women with T2D (65.9 ± 6.8%) than those health controls (59.5 ± 6.1%, $P = 0.009$) in unadjusted models, and this difference remained statistically significant after adjusting for multiple covariates. Lumbar spine, femur neck and total hip BMD values were similar between diabetic and nondiabetic women ($P > 0.05$).

There was a consistent inverse association between the vertebral PDFF and DXA-based BMD of the lumbar spine, femoral neck and total hip ($r = -0.503$~0.644, $P < 0.05$ for all). We further carried out correlation analyses between the PDFF and BMD with glucose or lipid metabolic indexes (Table 2). PDFF had a positive association with HbA1c and HOMA-IR but not with fasting plasma glucose and insulin. PDFF was also positively correlated with triglyceride and negatively with high-density lipoprotein cholesterol. There was no association between the PDFF and total cholesterol or low-density lipoprotein cholesterol. BMD at the total hip, femoral neck and lumbar spine was negatively correlated with HbA1c, HOMA-IR and triglyceride levels. Fasting plasma glucose, insulin levels, total cholesterol and low-density lipoprotein cholesterol showed no relation to BMD at the three sites. The least square means of PDFF or BMD were compared across quartiles of HOMA-IR after adjusting for age, BMI, alcohol intake, tobacco use, physical activity, serum lipids profile, whole body fat mass, lean mass and BMD (in PDFF comparisons) or PDFF (in BMD comparisons). As shown in Fig. 1, the vertebral PDFF was significantly increased in higher HOMA-IR quartiles compared to lower quartiles (P for trend < 0.001). We also observed this decreasing trend for mean BMD at the lumbar spine, femoral neck and total hip as the quartiles of HOMA-IR increased (P for trends < 0.05). The representative CSE-MRI of the lumbar spine from the women across HOMA-IR quartiles are presented in Fig. 2.

3.4. Association of logarithm-transformed HOMA-IR with PDFF

In multivariate linear regression models, logarithm-transformed HOMA-IR had a positive association with PDFF after adjustment for age, BMI, alcohol intake, tobacco use, physical activity, and serum lipids profile (model 1) (Standardized β coefficient ± standard error [β ± SE] = 0.382 ± 0.131, $P < 0.001$). The positive association of HOMA-IR with PDFF remained robust when whole body fat mass and lean mass entered into multivariate model (model 2) (β ± SE = 0.293 ± 0.128, $P = 0.002$). Further adjustment for BMD (model 3) did not alter the results observed in model 2 (β ± SE = 0.251 ± 0.123, $P = 0.011$).

4. Discussion

The published studies on the relationships between BMD phenotypes and glucose homeostasis are controversial. Although animal experiments demonstrated that insulin stimulated osteoblast proliferation and increased histomorphometric indices of bone formation [27], insulin signaling in osteoblasts also promoted bone resorption in *ex vivo* study [28]. In observation studies, insulin resistance had a positive [4,29,30], negative [31–34] or no [35] association with bone health. Bone density measurements underestimate skeletal fragility in T2D, which leads to the concept that insulin resistance might in part directly contribute to deficit of bone microstructure and material properties

Table 1
Baseline characteristics of the study subjects.

	T2D (n = 75)	Controls (n = 20)	*P*-value[a]	HOMA-IR quartiles in T2D				
				Q1 (< 1.90; n = 20)	Q2 (1.9–2.19; n = 19)	Q3 (2.20–2.76; n = 19)	Q4 (≥2.76; n = 17)	*P*-value[b]
Age, years	59.3 ± 4.6	58.8 ± 5.7	> 0.05	58.9 ± 4.8	59.4 ± 5.1	59.2 ± 3.6	59.7 ± 5.0	> 0.05
Height, cm	158.5 ± 6.0	159.2 ± 6.8	> 0.05	158.1 ± 5.2	157.8 ± 6.8	158.6 ± 6.4	159.5 ± 5.0	> 0.05
Weight, kg	61.9 ± 8.3	61.1 ± 8.1	> 0.05	59.2 ± 6.8	60.5 ± 7.2	63.1 ± 9.1	64.7 ± 9.2	< 0.001
Body mass index, kg/m^2	24.7 ± 3.5	24.3 ± 4.2	> 0.05	23.7 ± 2.8	24.5 ± 3.7	25.1 ± 3.2	25.5 ± 3.8	< 0.001
Fat mass (kg)	22.5 ± 4.5	21.9 ± 4.8	> 0.05	21.1 ± 4.1	21.7 ± 4.3	23.2 ± 4.5	23.8 ± 4.9	< 0.001
Lean mass (kg)	36.7 ± 5.6	37.1 ± 6.1	> 0.05	35.3 ± 5.8	36.5 ± 5.2	37.1 ± 5.9	37.9 ± 5.4	0.004
Regular alcohol consumption, n (%)	6 (8%)	2 (10%)	> 0.05	2 (10%)	1 (5%)	2 (11%)	2 (12%)	> 0.05
Cigarette smokers, n (%)	4 (5%)	1 (5%)	> 0.05	2 (10%)	1 (5%)	1 (5%)	0	> 0.05
Physical activity (METs/wk)	10.9 ± 5.5	11.8 ± 6.6	> 0.05	10.1 ± 4.3	12.4 ± 6.5	11.1 ± 5.2	10.0 ± 5.4	> 0.05
Total cholesterol (mmol/L)	4.79 ± 1.69	4.66 ± 1.57	> 0.05	4.82 ± 1.74	4.57 ± 1.59	4.69 ± 1.62	4.86 ± 1.84	> 0.05
LDL cholesterol (mmol/L)	2.75 ± 0.87	2. 67 ± 0.90	> 0.05	2.59 ± 0.93	2.68 ± 0.90	2.97 ± 0.83	2.90 ± 0.80	> 0.05
HDL cholesterol (mmol/L)	1.13 ± 0.48	1.34 ± 0.46	0.029	1.30 ± 0.50	1.33 ± 0.54	1.04 ± 0.42	0.92 ± 0.45	0.011
Triglyceride (mmol/L)	1.49 ± 0.64	1.21 ± 0.59	0.015	1.13 ± 0.45	1.39 ± 0.55	1.61 ± 0.60	1.70 ± 0.71	0.008
HbA1c (%)	8.56 ± 1.20	5.34 ± 0.52	< 0.001	7.68 ± 0.95	7.93 ± 1.26	8.35 ± 1.13	8.94 ± 1.34	< 0.001
Fasting glucose, mmol/L	7.80 (7.62, 8.66)	5.20 (4.34, 5.75)	< 0.001	7.46 (7.38, 7.59)	7.75 (7.64, 7.78)	8.15 (7.86, 8.63)	8.97 (8.80, 11.47)	< 0.001
Insulin, μU/L	17.5 (15.3, 26.0)	11.3 (7.9, 14.8)	< 0.001	14.3 (12.8, 14.8)	16.8 (16.0, 17.4)	19.5 (18.9, 22.5)	35.8 (30.7, 37.8)	< 0.001
HOMA-IR	2.19 (1.90, 2.76)	1.53 (1.17, 1.94)	< 0.001	1.83 (1.80, 1.88)	1.99 (1.95, 2.11)	2.36 (2.31, 2.56)	4.60 (3.45, 5.20)	< 0.001

Data are presented as mean ± SD, median (interquartile range) or frequency (%) as appropriate.
HDL, high-density lipoprotein; HOMA-IR, homeostasis model assessment of insulin resistance; LDL, low-density lipoprotein; METs, metabolic equivalent of tasks; Q, quartile; HbA1c, glycosylated hemoglobin.
HOMA-IR was calculated from fasting plasma insulin and glucose levels by using HOMA Calculator Software (from the University of Oxford), with higher values indicating insulin resistance.
[a] *P*-value between the T2D and control groups was calculated by independent-sample *t*-test, Chi-squared test or non-parametric test.
[b] *P*-value represented the significance of the differences in mean values across all the quartiles in the T2D group as calculated by an ANOVA, Chi-squared test or non-parametric test.

Table 2
Correlation analysis between biochemical measures and PDFF or skeletal density in the T2D group.

	HOMA-IR	HbA1c (%)	Insulin, μU/L	Fasting glucose, mmol/L	Total cholesterol (mmol/L)	Triglyceride (mmol/L)	LDL-c (mmol/L)	HDL-c (mmol/L)
PDFF, %	0.574[a]	0.336[b]	0.108	0.064	0.091	0.401[b]	0.102	–0.289[b]
Total hip BMD, g/cm^2	–0.189[b]	–0.175[b]	–0.024	–0.088	–0.083	–0.149[b]	0.014	0.018
Femoral neck BMD, g/cm^2	–0.166[b]	–0.171[b]	0.009	–0.100	0.042	–0.160[b]	–0.045	0.027
Lumbar spine BMD, g/cm^2	–0.211[b]	–0.190[b]	–0.032	0.011	0.037	–0.203[b]	–0.070	0.155[b]

BMD, bone mineral density; HDL-c, high-density lipoprotein cholesterol; HOMA-IR, homeostasis model assessment of insulin resistance; LDL-c, low-density lipoprotein cholesterol; HbA1c, glycosylated hemoglobin; PDFF, proton density fat fraction.
[a] $P < 0.001$.
[b] $P < 0.05$.

rather than BMD [4,36]. The majority of studies showed that elevated HOMA-IR was associated with lower bone quality [4,33,36,37]. This indicates that the negative effect on bone strength has offset the apparently favorable effect in higher or normal BMD associated with insulin resistance.

Substantial evidence shows that diabetes may be a state of elevated marrow fat content. This increase in marrow fat is often linked to the deterioration of bone quality, although this relationship may not be causal [5]. Similar to previous studies [3,7,38], we found a negative association between the amount of marrow fat and BMD in postmenopausal women with T2D. We also found evidence that women with diabetes had a significantly higher vertebral marrow fat content than those without. These results were confirmed by another study conducted by Sheu et al. [3] who reported older men with diabetes had a higher marrow fat compared to non-diabetic controls. In contrast, work by other investigators suggests that marrow fat content was similar in the diabetic postmenopausal women and healthy controls [7], however levels of unsaturated fatty acids in bone marrow was lower in diabetic subjects. Similar results were reported by Patsch et al. [8] who found no correlation between diabetic status and vertebral marrow adiposity, whereas T2D patients with prevalent fragility fractures had lower unsaturated marrow lipids and higher saturated fatty acids than non-diabetic women or diabetic non-fracture controls. Araujo et al. [9] also did not find a difference in vertebral marrow adiposity among T2D, obesity and healthy controls, but again marrow fat was positively associated with HbA1c levels. Despite no significant difference in marrow fat content between diabetic and nondiabetic obese women at baseline, weight loss from Roux-en-Y gastric bypass surgery reduced marrow fat content after 6 months only in diabetic women but not in the non-diabetic patients [39]. These inconsistent results may be attributed to 1) the heterogeneity of the investigated population while the gender, age and menopause status have been identified as important factors influencing bone marrow fat [40,41]; 2) the small sample size; and 3) the impact of therapeutic interventions such as thiazolidinediones or different covariates adjusted in the statistical analysis.

The mechanisms underlying skeletal fragility in diabetes are not completely understood. Numerous factors that are pertinent to the diabetic context have been shown to enhance marrow adipogenesis via

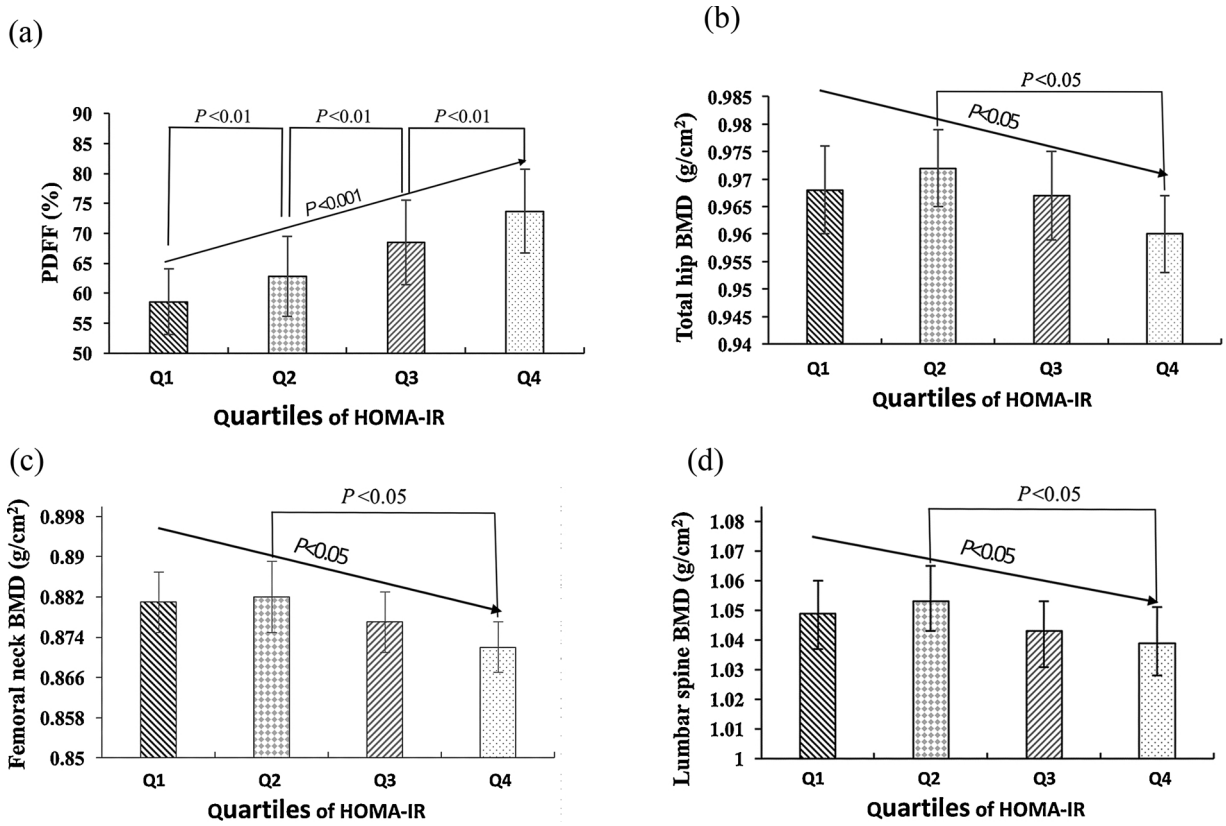

Fig. 1. Adjusted least square mean values of PDFF in subjects with diabetes across quartiles of HOMA-IR.
Data are expressed as means ± SD and were adjusted for age, body mass index, alcohol intake, tobacco use, physical activity, serum lipids profile, whole body fat mass, lean mass and BMD for PDFF comparisons or PDFF for BMD comparisons.
The bars from left to right are quartiles 1, 2, 3, and 4 of HOMA-IR.
The arrow indicates a significant linear trend between HOMA-IR quartile groups and PDFF values.
BMD, bone mineral density; HOMA-IR, homeostasis model assessment of insulin resistance; PDFF, proton density fat fraction.

disrupting the homeostatic balance between osteogenic and adipogenic differentiation of mesenchymal progenitor cells, including insulin, insulin-like growth factor-1 and tumor necrosis factor-α [1]. Additionally, long-standing hyperglycemia is linked to changes in marrow cellularity. High glucose microenvironment inhibits the proliferation and migration of bone mesenchymal stem cells, and hyperglycemia promotes the selection of adipogenesis over osteoblastogenesis of bone marrow stromal cells [42]. As a result, diabetic bone loss may be attributed to the “obesity” of bone.

Marrow fat is an active dynamic depot that vigorously contributes to local and systemic metabolic processes; however, its association with insulin resistance has not been consistently reported. A novel finding of our study is that newly diagnosed T2D postmenopausal women who had elevated insulin resistance showed marrow fat expansion irrespective of body compositions. Indeed, some [10], but not all [11,12] studies have reported a positive association between marrow fat expansion and insulin resistance. Intriguingly, marrow fat content was negatively associated with fasting insulin and HOMA-IR in obese and non-obese premenopausal women [11]. In other studies, no such association was found. Bani Hassan et al. [43] reported no associations between marrow fat content and serum glucose, inflammatory markers or insulin resistance indicators in a population of older men. The present data also seem to conflict with those obtained in young healthy adults with normal insulin sensitivity, non-diabetic women and subjects with T2D, in which no relationship was observed between marrow fat content and insulin or HOMA-IR [9,12,13]. It should be noted that severe and a long duration of diabetes appear to alter marrow fat and bone metabolism, structure, and strength, and then to increase skeletal fragility. Unfortunately, most previous studies did not evaluate the onset, duration, or severity of diabetes, or the use of antidiabetic medications, which may account for the conflicting results.

This study has several strengths. First, we used a relatively larger sample size of postmenopausal women as compared with previous studies, which enabled us to assess properly the relationship of glucose metabolism with marrow fat phenotype. More importantly, we only focused on newly diagnosed T2D, which ensured the homogeneity of the study sample to avoid potential influences of anti-diabetic medications on marrow fat content. In addition, we presented a new approach to the assessment of marrow PDFF in T2D using CSE-MRI. However, marrow fat fraction was so far primarily obtained by using single-voxel MR spectroscopy at a single lumbar vertebral level, and most of the previous studies quantifying the bone marrow fat fraction employed a single-TE MR spectroscopy measurement and did not perform any T2 correction, thus yielding the T2-weighted fat fraction but not the PDFF [11,21]. Due to the anatomical variation of the vertebral marrow composition, a spatially resolved PDFF map derived from CSE-MRI is advantageous in comparison with MR spectroscopy-based fat fraction measurements [20,44].

Our study has several limitations. First, the cross-sectional design did not allow us to establish causal relationship between insulin resistance and marrow adiposity. Longitudinal studies are needed to determine the temporal association between insulin resistance and marrow fat levels. Second, since this study was limited to postmenopausal females with newly diagnosed T2D, caution should be exercised in generalizing the results. Finally, high resolution quantitative CT for evaluating bone quality and more specific biomarkers of bone turnover were not available, and thus further studies are recommended.

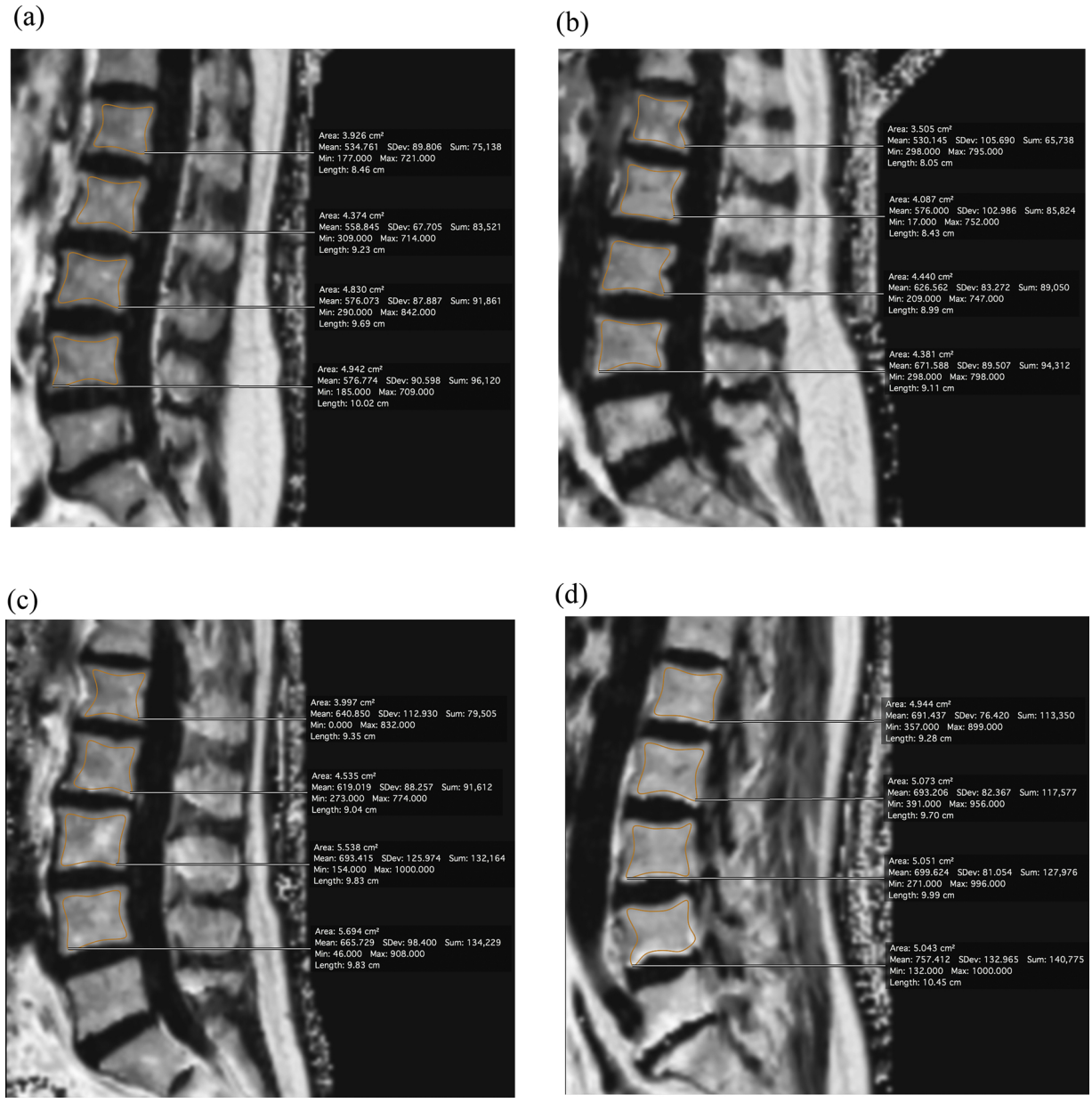

Fig. 2. Assessment of PDFF derived from eight-echo CSE-MRI across HOMA-IR quartiles.
(a)–(d) corresponds to quartiles 1, 2, 3, and 4 of HOMA-IR, respectively. Compared to lower quartiles (a, a 61.0-year-old woman with quartile 1 of HOMA-IR [mean PDFF: 56.2%]; b, a 61.3-year-old woman with quartile 2 of HOMA-IR [mean PDFF: 60.1%]), the vertebral PDFF was significantly increased in higher HOMA-IR quartiles (c, a 60.8-year-old woman with quartile 3 of HOMA-IR [mean PDFF: 65.5%]; d, a 60.5-year-old woman with quartile 4 of HOMA-IR [mean PDFF: 71.0%]). HOMA-IR, homeostasis model assessment of insulin resistance; PDFF, proton density fat fraction.

5. Conclusion

Our data reveal that a clear negative correlation was evident between marrow adiposity and BMD in postmenopausal women with newly diagnosed T2D, and those with elevated insulin resistance showed marrow fat expansion irrespective of body compositions. CSE-MRI helps clinicians to understand more about the links between marrow adipogenesis and insulin resistance or diabetes, providing insight into the paradoxical relationship among bone mass, fracture risk and diabetes. Further studies are needed to clarify whether marrow fat expansion precedes, follows, or parallels insulin resistance in T2D.

Funding

This work has received funding by the Shanghai Health and Family Planning Commission (201840034), National Natural Science Foundation of China (81874497), and Yueyang Hospital of Integrated Traditional Chinese and Western Medicine (2017YJ13).

Conflict of interest

All authors declare that they have no conflict of interest.

Acknowledgements

We would like to thank Dr. Dan Shi, Dr.Miao Li and Dr.Wei Fang for their assistance with data collection and image acquisition. The technical help from Dr. Qingjiao Zhang and Dr. Xiaoting Hu for performing the DXA scans is very much appreciated. We also thank Maki Polat, PhD, School of Medicine and Public Health, University of Wisconsin, for

giving valuable suggestions for study design.

References

[1] A. Palermo, L. D'Onofrio, R. Buzzetti, S. Manfrini, N. Napoli, Pathophysiology of bone fragility in patients with diabetes, Calcif. Tissue Int. 100 (2) (2017) 122–132.

[2] J. Tan, L. Zhou, Y. Zhou, et al., The influence of diabetes mellitus on proliferation and osteoblastic differentiation of MSCs, Curr. Stem Cell Res. Ther. 12 (5) (2017) 388–400.

[3] Y. Sheu, F. Amati, A.V. Schwartz, et al., Vertebral bone marrow fat, bone mineral density and diabetes: the osteoporotic fractures in men (MrOS) study, Bone 97 (2017) 299–305.

[4] J. Yang, N. Hong, J.S. Shim, Y. Rhee, H.C. Kim, Association of insulin resistance with lower bone volume and strength index of the proximal femur in nondiabetic postmenopausal women, J. Bone Metab. 25 (2) (2018) 123–132.

[5] A.G. Veldhuis-Vlug, C.J. Rosen, Clinical implications of bone marrow adiposity, J. Intern. Med. 283 (2) (2018) 121–139.

[6] A. Krings, S. Rahman, S. Huang, Y. Lu, P.J. Czernik, B. Lecka-Czernik, Bone marrow fat has brown adipose tissue characteristics, which are attenuated with aging and diabetes, Bone 50 (2) (2012) 546–552.

[7] T. Baum, S.P. Yap, D.C. Karampinos, et al., Does vertebral bone marrow fat content correlate with abdominal adipose tissue, lumbar spine bone mineral density, and blood biomarkers in women with type 2 diabetes mellitus? J. Magn. Reson. Imaging 35 (1) (2012) 117–124.

[8] J.M. Patsch, X. Li, T. Baum, et al., Bone marrow fat composition as a novel imaging biomarker in postmenopausal women with prevalent fragility fractures, J. Bone Miner. Res. 28 (8) (2013) 1721–1728.

[9] I.M. de Araujo, C.E. Salmon, A.K. Nahas, M.H. Nogueira-Barbosa, J. Elias Jr., F.J. de Paula, Marrow adipose tissue spectrum in obesity and type 2 diabetes mellitus, Eur. J. Endocrinol. 176 (1) (2017) 21–30.

[10] G. Li, Z. Xu, H. Lin, Y. Chen, X. Li, S. Chang, Association between insulin resistance and the magnetic resonance spectroscopy-determined marrow fat fraction in non-diabetic postmenopausal women, Menopause 25 (6) (2018) 676–682.

[11] F. Ermetici, S. Briganti, A. Delnevo, et al., Bone marrow fat contributes to insulin sensitivity and adiponectin secretion in premenopausal women, Endocrine 59 (2) (2018) 410–418.

[12] F.J. de Paula, I.M. de Araujo, A.L. Carvalho, J. Elias Jr., C.E. Salmon, M.H. Nogueira-Barbosa, The relationship of fat distribution and insulin resistance with lumbar spine bone mass in women, PLoS One 10 (6) (2015) e0129764.

[13] N. Di Iorgi, S.D. Mittelman, V. Gilsanz, Differential effect of marrow adiposity and visceral and subcutaneous fat on cardiovascular risk in young, healthy adults, Int. J. Obes. (Lond.) 32 (12) (2008) 1854–1860.

[14] E.L. Scheller, W.P. Cawthorn, A.A. Burr, M.C. Horowitz, O.A. MacDougald, Marrow adipose tissue: trimming the fat, Trends Endocrinol. Metab. 27 (6) (2016) 392–403.

[15] T.A. Walji, S.E. Turecamo, A.C. Sanchez, et al., Marrow adipose tissue expansion coincides with insulin resistance in MAGP1-Deficient mice, Front. Endocrinol. (Lausanne) 7 (2016) 87.

[16] G. Li, Z. Xu, A. Zhuang, et al., Magnetic resonance spectroscopy-detected change in marrow adiposity is strongly correlated to postmenopausal breast cancer risk, Clin. Breast Cancer 17 (3) (2017) 239–244.

[17] G. Li, Z. Xu, H. Gu, et al., Comparison of chemical shift-encoded water-fat MRI and MR spectroscopy in quantification of marrow fat in postmenopausal females, J. Magn. Reson. Imaging 45 (1) (2017) 66–73.

[18] F. Schick, H. Bongers, W.I. Jung, et al., Proton relaxation times in human red bone marrow by volume selective magnetic resonance spectroscopy, Appl. Magn. Reson. 3 (6) (1992) 947–963.

[19] C.S. Gee, J.T. Nguyen, C.J. Marquez, et al., Validation of bone marrow fat quantification in the presence of trabecular bone using MRI, J. Magn. Reson. Imaging 42 (2) (2015) 539–544.

[20] T. Baum, A. Rohrmeier, J. Syvari, et al., Anatomical variation of age-related changes in vertebral bone marrow composition using chemical shift encoding-based water-fat magnetic resonance imaging, Front. Endocrinol. (Lausanne) 9 (2018) 141.

[21] F.C. Schmeel, J.A. Luetkens, S.J. Enkirch, et al., Proton density fat fraction (PDFF) MR imaging for differentiation of acute benign and neoplastic compression fractures of the spine, Eur. Radiol. (2018), https://doi.org/10.1007/s00330-018-5513-0.

[22] H. Yu, S.B. Reeder, A. Shimakawa, J.H. Brittain, N.J. Pelc, Field map estimation with a region growing scheme for iterative 3-point water-fat decomposition, Magn. Reson. Med. 54 (4) (2005) 1032–1039.

[23] S. Ruschke, H. Eggers, H. Kooijman, et al., Correction of phase errors in quantitative water-fat imaging using a monopolar time-interleaved multi-echo gradient echo sequence, Magn. Reson. Med. 78 (3) (2017) 984–996.

[24] H. Yu, A. Shimakawa, C.A. McKenzie, E. Brodsky, J.H. Brittain, S.B. Reeder, Multiecho water-fat separation and simultaneous R2* estimation with multi-frequency fat spectrum modeling, Magn. Reson. Med. 60 (5) (2008) 1122–1134.

[25] D.C. Karampinos, S. Ruschke, M. Dieckmeyer, et al., Modeling of T2 * decay in vertebral bone marrow fat quantification, NMR Biomed. 28 (11) (2015) 1535–1542.

[26] M. Dieckmeyer, S. Ruschke, C. Cordes, et al., The need for T(2) correction on MRS-based vertebral bone marrow fat quantification: implications for bone marrow fat fraction age dependence, NMR Biomed. 28 (4) (2015) 432–439.

[27] J. Cornish, K.E. Callon, I.R. Reid, Insulin increases histomorphometric indices of bone formation in vivo, Calcif. Tissue Int. 59 (6) (1996) 492–495.

[28] M. Ferron, J. Wei, T. Yoshizawa, et al., Insulin signaling in osteoblasts integrates bone remodeling and energy metabolism, Cell 142 (2) (2010) 296–308.

[29] E.M. Dennison, H.E. Syddall, A. Aihie Sayer, S. Craighead, D.I. Phillips, C. Cooper, Type 2 diabetes mellitus is associated with increased axial bone density in men and women from the Hertfordshire Cohort Study: evidence for an indirect effect of insulin resistance? Diabetologia 47 (11) (2004) 1963–1968.

[30] V.V. Shanbhogue, J.S. Finkelstein, M.L. Bouxsein, E.W. Yu, Association between insulin resistance and bone structure in nondiabetic postmenopausal women, J. Clin. Endocrinol. Metab. 101 (8) (2016) 3114–3122.

[31] S.H. Ahn, H. Kim, B.J. Kim, S.H. Lee, J.M. Koh, Insulin resistance and composite indices of femoral neck strength in Asians: the fourth Korea National Health and Nutrition Examination Survey (KNHANES IV), Clin. Endocrinol. (Oxf.) 84 (2) (2016) 185–193.

[32] C. Verroken, H.G. Zmierczak, S. Goemaere, J.M. Kaufman, B. Lapauw, Insulin resistance is associated with smaller cortical bone size in nondiabetic men at the age of peak bone mass, J. Clin. Endocrinol. Metab. 102 (6) (2017) 1807–1815.

[33] M. Iki, Y. Fujita, K. Kouda, et al., Hyperglycemia is associated with increased bone mineral density and decreased trabecular bone score in elderly Japanese men: the Fujiwara-kyo osteoporosis risk in men (FORMEN) study, Bone 105 (2017) 18–25.

[34] D. Shin, S. Kim, K.H. Kim, K. Lee, S.M. Park, Association between insulin resistance and bone mass in men, J. Clin. Endocrinol. Metab. 99 (3) (2014) 988–995.

[35] E.W. Yu, M.S. Putman, N. Derrico, G. Abrishamanian-Garcia, J.S. Finkelstein, M.L. Bouxsein, Defects in cortical microarchitecture among African-American women with type 2 diabetes, Osteoporos. Int. 26 (2) (2015) 673–679.

[36] J.H. Kim, H.J. Choi, E.J. Ku, et al., Trabecular bone score as an indicator for skeletal deterioration in diabetes, J. Clin. Endocrinol. Metab. 100 (2) (2015) 475–482.

[37] V.N. Shah, R. Sippl, P. Joshee, et al., Trabecular bone quality is lower in adults with type 1 diabetes and is negatively associated with insulin resistance, Osteoporos. Int. 29 (3) (2018) 733–739.

[38] T.Y. Kim, A.V. Schwartz, X. Li, et al., Bone marrow fat changes after gastric bypass surgery are associated with loss of bone mass, J. Bone Miner. Res. 32 (11) (2017) 2239–2247.

[39] A.L. Schafer, X. Li, A.V. Schwartz, et al., Changes in vertebral bone marrow fat and bone mass after gastric bypass surgery: a pilot study, Bone 74 (2015) 140–145.

[40] D. Martel, B. Leporq, M. Bruno, R.R. Regatte, S. Honig, G. Chang, Chemical shift-encoded MRI for assessment of bone marrow adipose tissue fat composition: pilot study in premenopausal versus postmenopausal women, Magn. Reson. Imaging 53 (2018) 148–155.

[41] V. Pansini, A. Monnet, J. Salleron, P. Hardouin, B. Cortet, A. Cotten, 3 Tesla (1) H MR spectroscopy of hip bone marrow in a healthy population, assessment of normal fat content values and influence of age and sex, J. Magn. Reson. Imaging 39 (2) (2014) 369–376.

[42] A. Wang, R.J. Midura, A. Vasanji, A.J. Wang, V.C. Hascall, Hyperglycemia diverts dividing osteoblastic precursor cells to an adipogenic pathway and induces synthesis of a hyaluronan matrix that is adhesive for monocytes, J. Biol. Chem. 289 (16) (2014) 11410–11420.

[43] E. Bani Hassan, O. Demontiero, S. Vogrin, A. Ng, G. Duque, Marrow adipose tissue in older men: association with visceral and subcutaneous fat, bone volume, metabolism, and inflammation, Calcif. Tissue Int. 103 (2) (2018) 164–174.

[44] T.J.P. Bray, A. Bainbridge, S. Punwani, Y. Ioannou, M.A. Hall-Craggs, Simultaneous quantification of bone edema/adiposity and structure in inflamed bone using chemical shift-encoded MRI in spondyloarthritis, Magn. Reson. Med. 79 (2) (2018) 1031–1042.